Turkish Journal of Medical Sciences

Volume 47 | Number 5 Article 47

1-1-2017

Effects of valproic acid on sympathetic activity and left ventricularmyocardial remodelling in rats during pressure overload

YANG LIU

SIYU LI

ZHIGANG ZHANG

ZHANJUN LV

HUIJIE JIANG

See next page for additional authors

Follow this and additional works at: https://journals.tubitak.gov.tr/medical

 Part of the Medical Sciences Commons

Recommended Citation

LIU, YANG; LI, SIYU; ZHANG, ZHIGANG; LV, ZHANJUN; JIANG, HUIJIE; TAN, XIAO; and LIU, FENGQUAN (2017) "Effects of valproic acid on sympathetic activity and left ventricularmyocardial remodelling in rats during pressure overload," *Turkish Journal of Medical Sciences*: Vol. 47: No. 5, Article 47. https://doi.org/10.3906/sag-1704-142

Available at: https://journals.tubitak.gov.tr/medical/vol47/iss5/47

This Article is brought to you for free and open access by TÜBİTAK Academic Journals. It has been accepted for inclusion in Turkish Journal of Medical Sciences by an authorized editor of TÜBİTAK Academic Journals. For more information, please contact academic.publications@tubitak.gov.tr.

Effects of valproic acid on sympathetic activity and left ventricularmyocardial remodelling in rats during pressure overload

Authors
YANG LIU, SIYU LI, ZHIGANG ZHANG, ZHANJUN LV, HUIJIE JIANG, XIAO TAN, and FENGQUAN LIU

This article is available in Turkish Journal of Medical Sciences: https://journals.tubitak.gov.tr/medical/vol47/iss5/47

TÜBİTAK

Turkish Journal of Medical Sciences

http://journals.tubitak.gov.tr/medical/

Research Article

Turk J Med Sci
(2017) 47: 1651-1660
© TÜBİTAK
doi:10.3906/sag-1704-142

Effects of valproic acid on sympathetic activity and left ventricular myocardial remodelling in rats during pressure overload

Yang LIU[1,*], Siyu LI[2], Zhigang ZHANG[3], Zhanjun LV[2], Huijie JIANG[2], Xiao TAN[2], Fengquan LIU[1]

[1]Department of Internal Medicine, Affiliated Hospital of Northeast Agricultural University, Harbin, P.R. China

[2]College of Veterinary Medicine, Northeast Agricultural University, Harbin, P.R. China

[3]Heilongjiang Key Laboratory for Laboratory Animals and Comparative Medicine, Northeast Agricultural University, Harbin, P.R. China

Received: 25.04.2017 • **Accepted/Published Online:** 20.06.2017 • **Final Version:** 13.11.2017

Background/aim: Pressure overload induces cardiac remodelling and results in heart failure. Enhanced sympathetic outflow participates in the development of cardiac remodelling for the duration of pressure overload as an independent factor. Valproic acid has recently been shown to reduce neuronal injury and have antiinflammatory and antiapoptotic effects as a histone deacetylase inhibitor. We speculate that the drug plays a specific role in alleviating cardiac remodelling by inhibiting sympathetic activity.

Materials and methods: Surgery of partial abdominal aortic constriction was performed on male Sprague-Dawley rats. After 4 weeks, animal models of pressure overload were validated and then valproic acid (300 mg/kg) was administrated to rats once a day for the next 4 weeks. Experimental parameters were detected 4 weeks after validation.

Results: The administration of valproic acid alleviated cardiomyocyte hypertrophy, myocardial interstitial fibrosis and left ventricular diastolic dysfunction caused by partial abdominal aortic constriction. Valproic acid reduced the levels of plasma and local norepinephrine, augmented concentrations of hypothalamic gamma-aminobutyric acid, and had no side effects on the hepatic and renal function of the animals.

Conclusion: These results suggest that valproic acid may be a safe and effective therapeutic strategy for the inhibition of sympathetic outflow and cardiac remodelling.

Key words: Valproic acid, sympathetic activity, left ventricular myocardial remodelling, pressure overload, norepinephrine, gamma-aminobutyric acid

1. Introduction

Pressure overload on the heart leads to initial compensatory hypertrophy or myocardial interstitial fibrosis, and eventually results in decompensatory heart failure (1). Recent studies demonstrate that sympathetic overactivity exacerbates pressure overload-induced cardiac remodelling and contributes to the related cardiac diastolic dysfunction during the pressure overload (2,3). Levels of the adrenergic neurotransmitter norepinephrine (NE) released from sympathetic terminals reflect sympathetic activity.

Valproic acid (2-propylpentanoic acid sodium salt, VPA), commonly used to treat seizures and mood disorders, has recently been shown to reduce neuronal injury and have antiinflammatory and cardioprotective effects as a histone deacetylase inhibitor in many different rat models (4–6). Previous studies demonstrated VPA could reduce synthesis of catecholamines in the cerebral cortex of animals or level of plasma NE in humans via its various gamma-aminobutyric acid (GABA)-ergic actions (7,8). These findings suggest a new perspective to understand the cardioprotective effects of VPA and explain the central effects of this drug as a GABA-receptor agonist on sympathetic outflow.

Based on the few reports of the effects of VPA on the sympathetic activity and pressure overload-induced cardiac remodelling, we designed a study to verify the hypothesis that VPA could alleviate cardiac remodelling by attenuating the sympathetic outflow and achieve a greater central GABAergic system effect. A method of partial abdominal aortic constriction (PAAC) was used to produce the pressure overload model, and the sympathetic activities were evaluated through examining the plasma and local NE levels after treatment with VPA. We also examined GABA levels in the hypothalamus, because GABA, an efficient inhibitory neurotransmitter,

* Correspondence: ayang6303110@sina.com

participates in the regulation of the sympathetic outflow of hypothalamic and cardiovascular activities (9–14).

2. Materials and methods

2.1. Animals and experimental design

A total of 120 healthy male adult Sprague-Dawley rats were provided by the Experimental Animal Center of the First Clinical Medical College of Harbin Medical University (Harbin, China). Our experiments conformed to the Regulations for the Administration of Affairs Concerning Experimental Animals, National Committee of Science and Technology of China and Instructive Notions with Respect to Caring for Laboratory Animals, the Ministry of Science and Technology of China, and were approved by the Ethics Committee for Experimental Research, Northeast Agricultural University.

The animals were kept under standard laboratory conditions (12 h light:12 h dark at 24 ± 3 °C) and the breeding room was well ventilated. Food and water were provided ad libitum. Water consumption, rat bodyweight, activities, and nutrition status were monitored daily during the experiments. The rats were kept under observation for 8 weeks. Sham-operated animals were divided into the following two groups: (1) Sham group or (2) Sham + VPA group. Four weeks after the surgery, PAAC-induced cardiac hypertrophy was validated using a colour ultrasound machine. Then all of the rats with PAAC were randomly divided into the following two experimental groups: (1) PAAC group and (2) PAAC + VPA group, using a computer-generated random number.

Valproic acid was purchased from Nankai Share Pharmaceutical Co. Ltd. (Inner Mongolia, China) and was reconstituted with normal saline (vehicle). After the validation, VPA (300 mg/kg) was administered via the tail vein once a day for the next 4 weeks to the Sham + VPA and PAAC + VPA groups. The VPA dose was determined according to previous reports, which investigated the neuroprotective effect of VPA in an animal model of ischaemic brain injury (15–18).

2.2. Treatment for partial abdominal aortic constriction

Mechanical constriction of the abdominal aorta has been used for many years to produce pressure overload-induced myocardial remodelling in a number of different species (19,20). The rats were anaesthetised with thiopentone sodium (35 mg/kg intraperitoneally). The depth of anaesthesia achieved was monitored using a positive toe and tail pinch, the respiration rate, and the degree of muscle relaxation. A 4- to 5-cm midline incision was made in the abdomen to expose the aorta between the diaphragm and celiac artery. The 40 silk suture was passed beneath the abdominal aorta and then placed around the middle of the aorta and tightened with a needle (0.7 mm diameter). The needle was withdrawn to leave the abdominal aorta partially constricted. The incision was sutured in layers and Neosporin antibiotic powder (GlaxoSmithKline, Shanghai, China) was applied locally to the sutured wound. Postoperatively, analgesic treatment was provided (a single local subcutaneous infusion of 0.1 mL of lidocaine) and a heating pad was used to provide supplemental heating until the rats fully recovered from the anaesthesia. Sham-operated animals underwent the same surgical procedures without PAAC. The rats were kept under observation for the next 4 weeks.

2.3. Blood and tissue samples assay

A blood sample was collected from the right carotid artery after haemodynamic measurements and stored in a tube containing ethylene diamine tetra acetic acid. The blood was centrifuged at 3000 × *g* for 15 min to separate the serum, and then stored at −80 °C until analysed. After blood collection was completed, an additional dose of pentobarbitone was given to the rats. With the rats under deep anaesthesia, the hearts were rapidly excised, washed of blood, trimmed of fat and weighed, then rapidly frozen in liquid nitrogen, and stored at −176 to −196 °C. Hypothalamic tissues were carefully removed and preserved until analysed. Concentrations of NE and GABA were measured using enzyme linked immunosorbent assay kits (Jianglai Biotechnology Company, Shanghai, China) as instructed by the manufacturer. The biochemical tests were performed by experienced laboratory assistants that were unaware of the group assignments for the animals and other laboratory test results.

2.4. Morphological assessments

Excised tissue samples from the lateral wall of the left ventricle were prepared for haematoxylin and eosin (HE) staining. After staining, a light microscope (Olympus BX50 microscope, Tokyo Electronic Industry, Co., Ltd, Tokyo, Japan) connected to a personal computer was used to analyse cardiomyocyte diameter. To quantify cardiomyocyte size, digital images were captured of the cardiomyocyte cross-sectional area and measured using image analysis software (Image-Pro Plus, Media Cybernetics, Inc., Silver Spring, MD, USA). Twenty cells from two distinct sites were measured per sample. The average size of all measured cardiomyocytes within a sample was determined and expressed in units of cross-sectional area (in 2 μm). Only cardiomyocytes with a well-defined cellular membrane and visible nucleus were considered suitable for measurement.

Masson's Trichrome Stain was used for evaluation of interstitial fibrosis. Ventricular cardiac muscle stored in 70% ethanol was dehydrated, cleared, and embedded in paraffin. Routine 4 μm serial sectioning was performed, and slides were dried in a 60 °C oven. For Masson staining, slides were submerged in Masson's Trichrome solution (Harbin Medical University Pathology Laboratory,

Harbin, China) for 5 min and washed with 0.2% acetic acid for 10 s, followed by 5% phosphotungstic acid for 10 min. They were then washed twice with 0.2% acetic acid solution, stained with 2% aniline blue solution for 5 min, and washed twice with 0.2% acetic acid. The sections were dehydrated using gradient ethanol, cleared in xylene, and sealed using neutral Balsam. The quantification of the fibrotic area was analysed as a percentage of the total area using image analysis software.

2.5. Echocardiography and Doppler imaging

Four weeks after validation, the cardiac structure and function of rats in the four groups were evaluated. The rats were lightly anaesthetised (chloral hydrate) and then echocardiography was performed on the animals using a GE Vivid5 colour ultrasound machine (GE Vingmed; GE Healthcare Fairfield, CT, USA) with a linear 13 MHz probe. The left ventricular posterior wall (LVPW) thickness, the interventricular septum (IVS) thickness, the left ventricular internal dimensions at diastole and systole (LVIDd and LVIDs, respectively), and left ventricular ejection fraction were measured from the two-dimensional targeted M-mode echocardiographic tracings in the parasternal long-axis view at the level of the mitral leaflet tips. Left ventricular fractional shortening (LVFS) (1), relative wall thickness (RWT) (2), and left ventricular mass (LVM) (3) were calculated using the following formulae, respectively:

$$\mathrm{LVFS\%} = \frac{\mathrm{LVIDd\,(mm)} - \mathrm{LVIDs\,(mm)}}{\mathrm{LVIDd\,(mm)}} \times 100\% \quad (1)$$

$$\mathrm{RWT} = \frac{\mathrm{IVS\,(mm)} + \mathrm{LVPM\,(mm)}}{\mathrm{LVIDd\,(mm)}} \quad (2)$$

$$\mathrm{LVM(mg)} = 1.05 \times [\mathrm{IVS(mm)} + \mathrm{LVIDd(mm)} + \mathrm{LVPW(mm)}]^3 - \mathrm{LVIDd}^3\mathrm{(mm)} \quad (3)$$

Doppler imaging was used to record the transmitral peaks of early (E) and late (A) diastolic mitral inflow velocities at the tips of the mitral valve leaflets, rate of blood flow, and pressure gradient at the left ventricular outflow tract. The left atrial dimensions were used for excluding pseudo-normalization of E/A values.

2.6. Haemodynamic measurements

Four weeks after validation, the animals were anaesthetised with a sodium pentobarbitone solution (60 mg/kg, intraperitoneally). A fluid-filled polyethylene catheter connected to a RM-600 4–channel physiologic recorder (Nihon Kohden, Tokyo, Japan) was inserted into the right common carotid artery, which was then advanced into the left ventricular cavity and synchronously recorded the systolic pressures (LVSP), end-diastolic pressures (LVEDP), and the maximum rate of pressure rise and fall (dP/dt max and dP/dt min, respectively). All records were obtained at 2 kHz.

2.7. Biochemical detection

To assess the side effects of VPA, 4 weeks after treatment we examined the hepatic and renal function of rats, including concentrations of plasma aspartate aminotransferase, alanine aminotransferase, lactate dehydrogenase, creatinine, and blood urea nitrogen (BUN), which were measured using an automatic biochemical analyser, AU400 (Olympus, Tokyo, Japan).

2.8. Statistical analysis

Statistical analyses were performed using SPSS 20.0 (SPSS Inc., Chicago, IL, USA) and GraphPad Prism 5.0 (GraphPad Software Inc., San Diego, CA, USA). All results were expressed as mean ± SD. The data obtained from various groups were analysed using one-way analysis of variance followed by the Tukey or Dunnett's T3 test, as appropriate. $P < 0.05$ was considered to be statistically significant.

3. Results

A total of six rats died during the experiment. Four weeks after the surgery, 24/25 and 26/29 animals of the sham-operated and PAAC groups, respectively, were alive. At 8 weeks, 12/12, 12/12, 12/14, and 12/12 animals of the Sham, Sham + VPA, PAAC, and PAAC + VPA groups, respectively, were alive. The remaining rats without surgery or drug treatment were kept for standby.

3.1. The effects of VPA on ventricular weight

Eight weeks after surgery, heart wet weight (HWW) and HWW normalised to bodyweight (HWW/BW) were increased in the PAAC group compared with the Sham group ($P < 0.01$, $P < 0.01$, respectively), which reflects the presence of pressure overload-induced cardiac remodelling. The administration of VPA significantly decreased the HWW and HWW/BW ($P < 0.05$) (Table 1).

3.2. The effects of VPA on the echocardiographic parameters

Echocardiography was used to validate the PAAC procedure. Four weeks after surgery, the IVS thickness and the LVPW thickness significantly increased ($P < 0.05$). The LVIDd was decreased ($P < 0.05$). These results indicate that the PAAC procedure successfully established the animal model of cardiac remodelling (Table 2). Four weeks after validation, the Sham group, Sham + VPA group, PAAC group, and PAAC + VPA group exhibited similar left ventricular ejection fraction and left ventricular fractional shortening values, indicating that the overall systolic functions of the heart could still compensate for the enhanced afterload by PAAC. The administration of VPA inhibited the progress of myocardial remodelling from increasing IVS thickness and LVPW thickness, and from decreasing the LVIDd and E/A values. These results were supported by reduced relative wall thickness and left ventricular mass that were obtained from mathematical

Table 1. The heart wet weights at 8 weeks among the 4 groups.

Parameters	Sham	Sham + VPA	PAAC	PAAC + VPA
HWW (g)	0.90 ± 0.08	0.91 ± 0.07	1.29 ± 0.15**	1.01 ± 0.18$
BW (kg)	0.27 ± 0.01	0.26 ± 0.01	0.29 ± 0.01	0.27 ± 0.01
HWW/BW (g/kg)	3.33 ± 0.16	3.40 ± 0.18	4.49 ± 0.40$**	3.70 ± 0.21#*$

Abbreviations: HWW: heart wet weight; BW: body weight; n = 10 in each group. *P < 0.05, **P < 0.01 vs. Sham group; $P < 0.05 vs. PAAC group; #P < 0.05 vs. Sham + VPA group.

Table 2. Echocardiographic parameters at 4 weeks after partial abdominal aortic constriction.

Parameters	Sham	Sham + VPA	PAAC
IVS thickness (mm)	1.22 ± 0.20	1.24 ± 0.18	1.48 ± 0.24*#
LVPW thickness (mm)	1.23 ± 0.13	1.20 ± 0.17	1.41 ± 0.17*#
LVIDd (mm)	5.10 ± 0.28	5.00 ± 0.28	4.77 ± 0.33*
LVIDs (mm)	3.68 ± 0.25	3.71 ± 0.25	3.64 ± 0.23
LVEF (%)	62.34 ± 3.85	59.15 ± 2.81	54.18 ± 1.18
LVFS (%)	27.86 ± 2.39	25.84 ± 1.70	23.42 ± 6.58

Abbreviations: IVS: interventricular septum; LVPW: left ventricular posterior wall; LVIDs: left ventricular internal dimensions at systole; LVIDd: left ventricular internal dimensions at diastole; LVEF: left ventricular ejection fraction; LVFS: left ventricular fractional shortening. *P < 0.05 vs. Sham group; $P < 0.05 vs. PAAC group; #P < 0.05 vs. Sham + VPA group.

methods (Table 3; Figure 1). These findings suggest that VPA attenuates PAAC-induced cardiac remodelling.

HE staining revealed a higher cardiomyocyte cross-sectional area in the PAAC group compared with the Sham group (P < 0.05). The administration of VPA significantly reduced the cardiomyocyte cross-sectional area (P < 0.05), confirming that VPA treatment alleviates cardiomyocyte hypertrophy (Figures 2A and 2B).

3.3. The effects of VPA on the haemodynamic parameters

The changes in haemodynamic parameters developed in parallel with the changes in the echocardiographic parameters. The levels of LVEDP and LVSP were significantly higher in the PAAC group compared with the Sham group (P < 0.05). The administration of VPA lowered the increased LVEDP and LVSP (P < 0.05, P < 0.05, respectively). There were no significant differences in the level of dP/dt max among the four groups. The level of dP/dt min was significantly lower in the PAAC group compared with the Sham group (P < 0.05). VPA increased the level of dP/dt min (P < 0.05) (Table 4).

3.4. The effects of VPA on myocardial pathological changes

The extent of collagen hyperplasia was evaluated using Masson's Tricolor staining. A robust myocardial interstitial fibrosis with increased amounts of surrounding matrix was found in the Sham animals, indicating that the PAAC procedure induced cardiac collagen remodelling in addition to the cardiomyocyte hypertrophy. The administration of VPA improved the myocardial interstitial fibrosis (P < 0.05) (Figures 3A and 3B).

3.5. The effects of VPA on concentrations of plasma NE and local NE

PAAC induced an enhanced sympathetic outflow that was reflected by increased concentrations of plasma and local NE compared with the Sham groups (P < 0.05). However, sympathetic overexcitation was inhibited by VPA for the duration of the sustaining pressure overload (P < 0.05) (Figures 4A and 4B).

3.6. The effects of VPA on the concentrations of hypothalamic GABA

Concentrations of hypothalamic GABA decreased in the PAAC group compared with the Sham group (P < 0.05). The administration of VPA increased the concentration of hypothalamic GABA in the PAAC + VPA group (P < 0.05) (Figure 4C).

3.7. The effects of VPA on the biochemical parameters

There were no differences in serum concentrations of aspartate aminotransferase, alanine aminotransferase, lactate dehydrogenase, and creatinine among the

Table 3. The echocardiographic parameters at 8 weeks among the 4 groups.

Parameters	Sham	Sham + VPA	PAAC	PAAC + VPA
HR (beats/min)	306.9 ± 15.1	315.3 ± 22.3	322.9 ± 27.4	311.3 ± 20.0
LAd (mm)	38.2 ± 2.7	40.1 ± 2.4	47.2 ± 4.7*	42.1 ± 2.9
IVS thickness (mm)	1.12 ± 0.12	1.21 ± 0.10	1.90 ± 0.15*	1.53 ± 0.13*#$
LVPW thickness (mm)	1.15 ± 0.13	1.12 ± 0.11	1.82 ± 0.19*	1.45 ± 0.16*#$
LVIDd (mm)	5.30 ± 0.22	5.28 ± 0.23	4.76 ± 0.16*	5.17 ± 0.37$
LVIDs (mm)	3.98 ± 0.21	3.89 ± 0.19	3.76 ± 0.16	3.80 ± 0.23
LVEF (%)	57.66 ± 2.31	60.00 ± 1.68	50.26 ± 7.24*	59.73 ± 6.91
LVFS (%)	24.93 ± 1.38	26.33 ± 1.02	20.94 ± 3.90*	26.34 ± 3.90
E/A radio	1.72 ± 0.17	1.62 ± 0.18	0.58 ± 0.06*	1.59 ± 0.12$
LVOT, PG (mmHg)	0.46 ± 0.10	0.49 ± 0.08#	0.75 ± 0.33*	0.45 ± 0.13#
LVOT, BFR (cm/s)	0.33 ± 0.03	0.35 ± 0.03#	0.42 ± 0.09*	0.33 ± 0.06#
LVM (mg)	310.2 ± 60.6	318.8 ± 60.1	537.8 ± 101.5*	437.0 ± 98.3*#$
RWT	0.43 ± 0.03	0.44 ± 0.02	0.78 ± 0.46*	0.58 ± 0.04*#$

Abbreviations: LAd: left atrial dimension; LVOT: left ventricular outflow tract; PG: pressure gradient; BFR: blood flow rate; RWT: relative wall thickness; n = 10 in each group. *P < 0.05 vs. Sham group; $P < 0.05 vs. PAAC group; #P < 0.05 vs. Sham + VPA group.

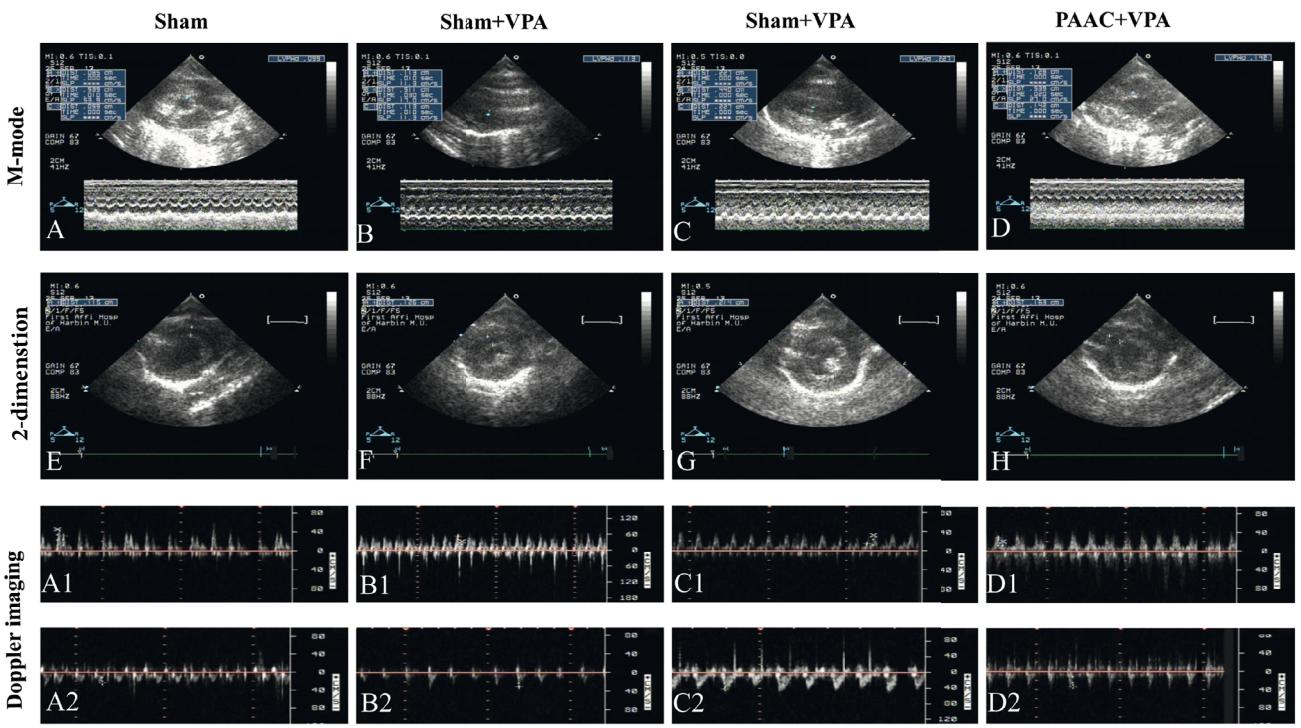

Figure 1. Echocardiography and Doppler imaging. The left ventricular posterior wall (LVPW) thickness, interventricular septum (IVS) thickness, and the left ventricular internal dimensions at diastole and systole (LVIDd and LVIDs, respectively) were measured from the two-dimensional targeted M-mode echocardiographic tracings in the parasternal long-axis view at the level of the mitral leaflet tips and apexes of LV. Doppler imaging was used to record the transmitral peaks of early (E) and late (A) diastolic mitral inflow velocities at the tips of the mitral valve leaflets, rate of blood flow, and pressure gradient at the left ventricular outflow tract.

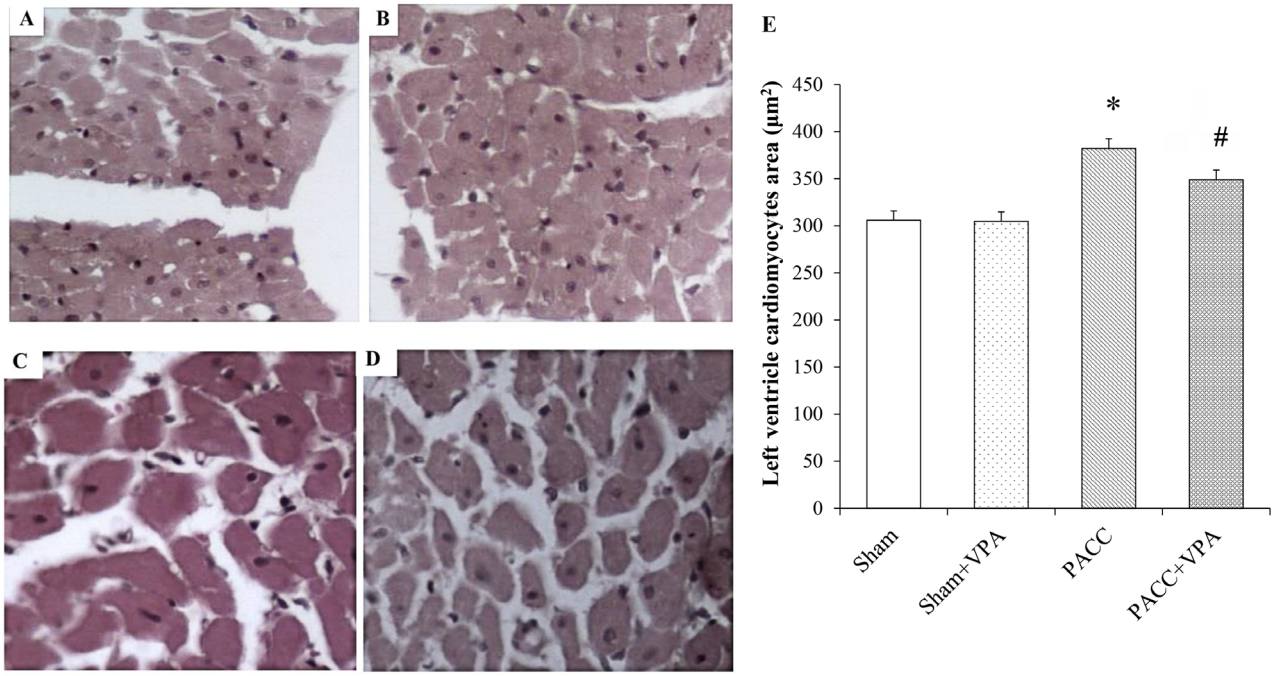

Figure 2. HE staining and morphological assessments (400×). Effects of VPA on cardiomyocyte size assessed by haematoxylin and eosin staining. Haematoxylin/eosin staining of transverse sections. (A) Sham group; (B) Sham + VPA group; (C) PACC group; (D) PACC+ VPA group; (E) Summary data for cross-sectional area of cardiac myocytes. Values are means ± SD, n = 12. *P < 0.05 versus Sham group; #P < 0.05 versus PAAC group.

Table 4. The hemodynamic parameters at 8 weeks among the 4 groups.

Parameters	Sham	Sham + VPA	PAAC	PAAC + VPA
LVSP (mmHg)	151.5 ± 3.9	149.2 ± 5.8	167.9 ± 6.8*	152.0 ± 3.2$
LVEDP (mmHg)	4.9 ± 0.5	4.4 ± 0.6	11.2 ± 1.4*	5.4 ± 0.3$
dP/dtmax (mmHg/s)	8053.1 ± 823.6	8040.6 ± 781.3	7972.4 ± 394.4	7788.9 ± 463.4
dP/dtmin (mmHg/s)	5665.5 ± 514.2	5786.3 ± 403.3	4648.8 ± 454.9*	5972.7 ± 5518.3$

Abbreviations: LVSP: left ventricular systolic pressure; LVEDP: left ventricular end-diastolic pressure; dP/dtmax and dP/dt min: the maximum rate of pressure rise and fall; n = 10 in each group. *P< 0.05 vs. Sham group; $P < 0.05 vs. PAAC group; #P < 0.05 vs. Sham + VPA group.

four groups. Compared with the PAAC group, serum concentrations of BUN were decreased in the PAAC + VPA group (P < 0.05) (Table 5).

4. Discussion

Cardiac remodelling was regarded as an adaptive response to an increased workload. However, clinical and experimental observations have shown that the degree of cardiac hypertrophy or interstitial fibrosis is not proportional to workload, which means that extra factors participate in the pathological process of cardiac remodelling (21). Overactivation of the sympathetic nervous system plays a pivotal role in hypertrophic remodelling by modulating the cardiovascular growth response; cardiac performance decreases as sympathetic activity increases. Emerging experimental evidence suggests that adrenaline receptor signalling contributes to the development of cardiac hypertrophy and fibrosis (22). Sympathectomy, which abolishes the collagen deposition and myocardial interstitial fibrosis of the left ventricle, has been implicated experimentally with aortic banding-induced pressure overload (23). In this study, PAAC produced significant cardiac hypertrophy, myocardial interstitial fibrosis, and left ventricular diastolic dysfunction as well as enhancement of sympathetic outflow. VPA exhibited an anti-remodelling effect, by

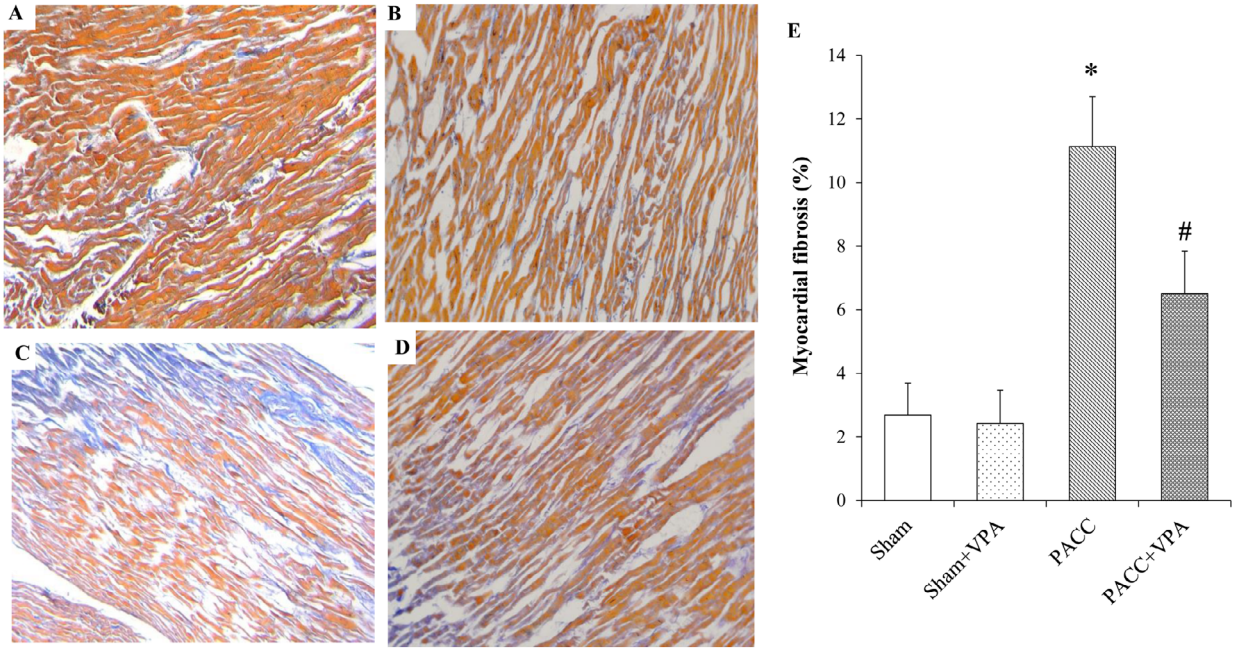

Figure 3. Masson staining and morphological assessments (200×). Effects of VPA on interstitial fibrosis assessed by Masson staining. Masson staining of transverse sections of left ventricle. Fibrotic area is stained blue. (A) Sham group; (B) Sham + VPA group; (C) PACC group; (D) PACC + VPA group; (E) Summary data for interstitial fibrosis area. Values are mean ± SD, n =12. *P < 0.05 versus Sham group; #P < 0.05 versus PAAC group.

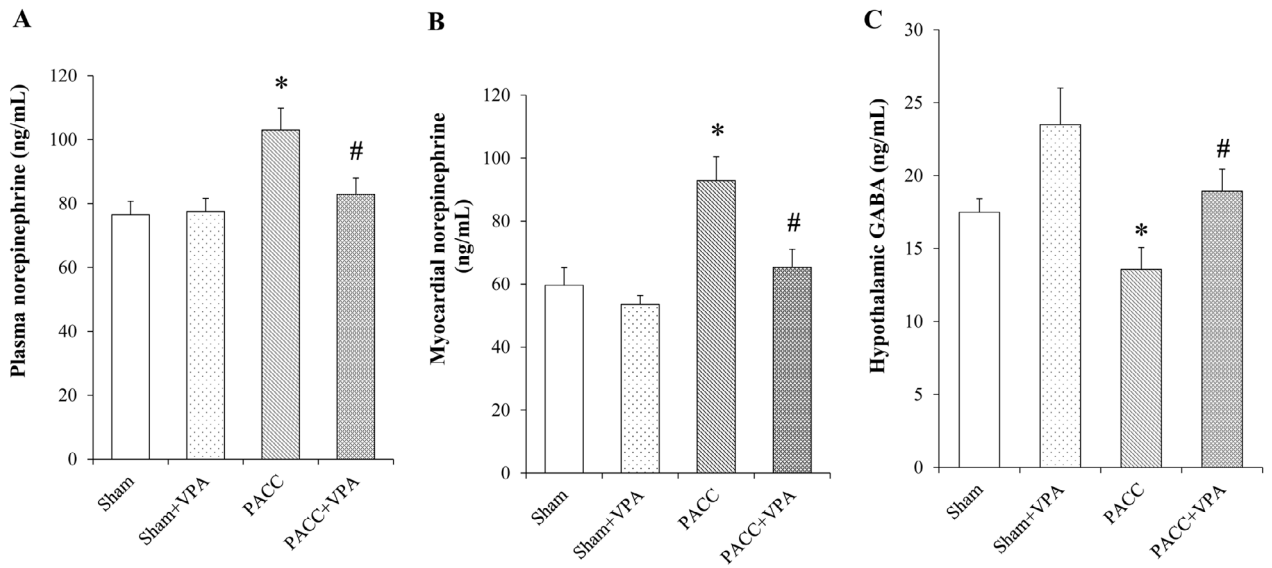

Figure 4. Blood and tissue samples assay. Blood and tissue samples from rats were detected using the double antibody sandwich method of ELISA. (A) Concentration of plasma NE; (B) Concentration of local NE; (C) Content of hypothalamic GABA. *P < 0.05 versus Sham group; #P < 0.05 versus PAAC group.

significantly decreasing normalised left ventricular weight, cardiomyocyte cross-sectional area, and myocardial fibrotic area. This was supported by the improvement of haemodynamic parameters and the reduction in plasma and local NE levels. These findings indicate that VPA is cardioprotective against PAAC-induced cardiac remodelling.

Increased sympathetic outflow may play a key role in the pathogenesis and maintenance of hypertension and heart failure, including pressure overload (2,3,24). However,

Table 5. The hepatic and renal function parameters at 8 weeks among the four groups.

Parameters	Sham	Sham + VPA	PAAC	PAAC + VPA
AST (U/L)	104.5 ± 11.7	109.2 ± 14.3	107.9 ± 22.7	107.0 ± 18.0
ALT (U/L)	34.0 ± 3.4	35.5 ± 4.6	36.1 ± 4.3	31.5 ± 5.5
LDH (U/L)	840.0 ± 336.1	839.1 ± 261.5	1054.5 ± 378.2	772.7 ± 343.2
CREA (μmol/L)	37.6 ± 5.1	38.9 ± 5.6	34.6 ± 5.4	33.6 ± 2.7
BUN (mmol/L)	8.2 ± 2.9	7.8 ± 2.1	10.1 ± 1.9	6.2 ± 2.4$

Abbreviations: AST: aspartate aminotransferase; ALT: alanine aminotransferase; LDH: lactate dehydrogenase; GREA: creatinine; BUN: blood urea nitrogen; n = 10 in each group; $P < 0.05 vs. PAAC group.

the mechanisms underlying heightened sympathetic outflow in hypertension remain poorly understood. Most studies on the central alterations in hypertensive animals have focused on the hypothalamus (25–27), which is an important brain region controlling sympathetic outflow and arterial blood pressure through projections to the intermediolateral cell column of the spinal cord and the rostral ventrolateral medulla (28–31). A lesion of the hypothalamus reduces sympathetic activity and attenuates the development of hypertension in experimental animals (32,33). The role of the hypothalamus in nerve action relies on many neurotransmitters, including glutamic acid and GABA. Modulating ambient GABA levels or the efficacy of GABAergic synaptic inputs in the hypothalamic pressor area tonically inhibits sympathetic outflow and arterial blood pressure (34–36). Therefore, regulation of GABA levels in the hypothalamus might be a potential target for inhibiting sympathetic outflow.

As a drug for the treatment of neurological disease, VPA can suppress neuronal activity by employing multiple neurochemical mechanisms. Regardless of the various opinions on the action of VPA on membrane ion channels, intracellular messenger systems, amino acid release, and metabolism of monoamines, the vast majority of researchers agree that the main neuropharmacological effect of this drug is the enhancement of GABAergic transmission and a rise in GABA levels in the central nervous system (37–43). In this study, a reduced GABA level in the hypothalamus was observed in the PAAC group, but VPA significantly boosted the GABA level in the region as well as sympathetic inhibition. Therefore, we speculate that the independent pharmacological effect of VPA on hypothalamic GABA levels contributes to reduced sympathetic activity and cardiac remodelling.

In forming the conclusions of this study, we recognise the straightforward effects of VPA on the heart as a histone deacetylase inhibitor, which were demonstrated in recent years (44,45). However, we suggest that VPA has multiple positive effects of cardiac remodelling, via regulation of sympathetic excitability through the central pathway.

The findings from this study indicate that VPA can effectively inhibit the sympathetic outflow, alleviate cardiac remodelling, and improve left ventricular function during pressure overload. Moreover, VPA also increases the GABA level in the hypothalamus, which might contribute to decreasing sympathetic outflow.

Acknowledgements

We sincerely thank professor Guang Xing Li (Northeast Agricultural University) and Wei Yu (Affiliated Hospital of Northeast Agricultural University) for their encouragement and advice, and Li Huang of Biovol Technology Company (Shanghai, China) for his helpful comments. This work was supported by the Heilongjiang Province Foundation for Young Scholars (QC2010057).

References

1. Givvimani S, Kundu S, Narayanan N, Armaghan F, Qipshidze N, Pushpakumar S, Vacek TP, Tyagi SC. TIMP-2 mutant decreases MMP-2 activity and augments pressure overload induced LV dysfunction and heart failure. Arch Physiol Biochem 2013; 119: 65-74.
2. Mancia G, Grassi G, Giannattasio C, Seravalle G. Sympathetic activation in the pathogenesis of hypertension and progression of organ damage. Hypertension 1999; 34: 724-728.
3. Dab H, Hachani R, Hodroj W, Sakly M, Bricca G, Kacem K. Differential control of collagen synthesis by the sympathetic and renin–angiotensin systems in the rat left ventricle. Auton Neurosci 2009; 151: 106-110.
4. Lee JH, Kim K, Jo YH, Lee SH, Kang C, Kim J, Park CJ, Kim MA, Lee MJ, Rhee JE. Effect of valproic acid on survival and neurologic outcomes in an asphyxial cardiac arrest model of rats. Resuscitation 2013; 84: 1443-1449.

5. Jin HB, Guo XM. Valproic acid ameliorates coxsackievirus-B3-induced viral myocarditis by modulating Th17/Treg imbalance. Virol J 2016; 13: 168.
6. Andreou AP, Shields KG, Goadsby PJ. GABA and valproate modulate trigeminovascular nociceptive transmission in the thalamus. Neurobiol Dis 2010; 37: 314-323.
7. Takebayashi M, Motohashi N, Saito H, Kagaya A, Yamawaki S. Effect of acute treatment with sodium valproate on catecholamine and serotonin synthesis in mouse cerebral cortex. Neuropsychobiology 1995; 32: 124-127.
8. Breum L, Astrup A, Gram L, Andersen T, Stokholm KH, Christensen NJ, Werdelin L, Madsen J. Metabolic changes during treatment with valproate in humans: implication for untoward weight gain. Metabolism 1992; 41: 666-670.
9. Tibiriçà E, Catelli M, Lessa MA, Roegel JC, Feldman J, Monassier L, Bousquet P. Inhibition of the centrally induced increases in myocardial oxygen demand in rabbits by chronic treatment with baclofen, a selective $GABA_B$ agonist. Br J Pharmacol 1995; 115: 1331-1335.
10. Jiang N, Shi P, Li HW, Lu S, Braseth L, Cuadra AE, Raizada MK, Sumners C. Phosphate-activated glutaminase-containing neurons in rat paraventricular nucleus express angiotensin type 1 receptors. Hypertension 2009; 54: 845-851.
11. Badoer E. Role of the hypothalamic PVN in the regulation of renal sympathetic nerve activity and blood flow during hyperthermia and in heart failure. Am J Physiol Renal Physiol 2010; 298: F839-F846.
12. Yang Z, Coote JH. Influence of the hypothalamic paraventricular nucleus on cardiovascular neurones in the rostral ventrolateral medulla of the rat. J Physiol 1998; 513: 521-530.
13. Blair ML, Piekut D, Want A, Olschowka JA. Role of the hypothalamic paraventricular nucleus in cardiovascular regulation. Clin Exp Pharmacol Physiol 1996; 23: 161-165.
14. Vaz GC, Bahia AP, de Figueiredo Müller-Ribeiro FC, Xavier CH, Patel KP, Santos RA, Moreira FA, Frézard F, Fontes MA. Cardiovascular and behavioral effects produced by administration of liposome-entrapped GABA into the rat central nervous system. Neuroscience 2015; 285: 60-69.
15. Kim HJ, Rowe M, Ren M, Hong JS, Chen PS, Chuang DM. Histone deacetylase inhibitors exhibit anti-inflammatory and neuroprotective effects in a rat permanent ischemic model of stroke: multiple mechanisms of action. J Pharmacol Exp Ther 2007; 321: 892-901.
16. Kabakus N, Ay I, Aysun S, Söylemezoglu F, Özcan A, Celasun B. Protective effects of valproic acid against hypoxic-ischemic brain injury neonatal rats. J Child Neurol 2005; 20: 582-587.
17. Ren M, Leng Y, Jeong M, Leeds PR, Chuang DM. Valproic acid reduces brain damage induced by transient focal cerebral ischemia in rats: potential roles of histone deacetylase inhibition and heat shock protein induction. J Neurochem 2004; 89: 1358-1367.
18. Wang ZF, Leng Y, Tsai LK, Leeds P, Chuang DM. Valproic acid attenuates blood-brain barrier disruption in a rat model of transient focal cerebral ischemia: the roles of HDAC and MMP-9 inhibition. J Cereb Blood Flow Metab 2011; 31: 52-57.
19. Balakumar P, Singh M. The possible role of caspase-3 in pathological and physiological cardiac hypertrophy in rats. Basic Clin Pharmacol Toxicol 2006; 99: 418-424.
20. Shimoyama M, Hayashi D, Takimoto E, Zou YZ, Oka T, Uozumi H, Kudoh S, Shibasaki F, Yazaki Y, Nagai R et al. Calcineurin plays a critical role in pressure overload-induced cardiac hypertrophy. Circulation 1999; 100: 2449-2454.
21. Obayashi M, Yano M, Kohno M, Kobayashi S, Tanigawa T, Hironaka K, Ryouke T, Matsuzaki M. Dose-dependent effect of ANG II-receptor antagonist on myocyte remodeling in rat cardiac hypertrophy. Am J Physiol 1997; 273: H1824-H1831.
22. Briest W, Hölzl A, Raßler B, Deten A, Leicht M, Baba HA, Zimmer HZ. Cardiac remodeling after long term norepinephrine treatment in rats. Cardiovasc Res 2001; 52: 265-273.
23. Perlini S, Palladini G, Ferrero I, Tozzi R, Fallarini S, Facoetti A, Nano R, Clari F, Busca G, Fogari R et al. Sympathectomy or doxazosin, but not propranolol, blunt myocardial interstitial fibrosis in pressure-overload hypertrophy. Hypertension 2005; 46: 1213-1218.
24. Allen AM. Inhibition of the hypothalamic paraventricular nucleus in spontaneously hypertensive rats dramatically reduces sympathetic vasomotor tone. Hypertension 2002; 39: 275-280.
25. Ito S, Komatsu K, Tsukamoto K, Kanmatsuse K, Sved AF. Ventrolateral medulla AT1 receptors support blood pressure in hypertensive rats. Hypertension 2002; 40: 552-559.
26. Esler M, Kaye D. Sympathetic nervous system activation in essential hypertension, cardiac failure and psychosomatic heart disease. J Cardiovasc Pharmacol 2000; 35: S1-S7.
27. Zhang K, Li YF, Patel KP. Reduced endogenous GABA-mediated inhibition in the PVN on renal nerve discharge in rats with heart failure. Am J Physiol Regul Integr Comp Physiol 2002; 282: R1006-R1015.
28. Hardy SGP. Hypothalamic projections to cardiovascular centers of the medulla. Brain Res 2001; 894: 233-240.
29. Pyner S, Coote JH. Identification of branching paraventricular neurons of the hypothalamus that project to the rostroventrolateral medulla and spinal cord. Neuroscience 2000; 100: 549-556.
30. Dampney RAL. Functional organization of central pathways regulating the cardiovascular system. Physiol Rev 1994; 74: 323-364.
31. Swanson LW, Sawchenko PE. Hypothalamic integration: organization of the paraventricular and supraoptic nuclei. Annu Rev Neurosci 1983; 6: 269-324.
32. Takeda K, Buñag RD. Augmented sympathetic nerve activity and pressor responsiveness in DOCA hypertensive rats. Hypertension 1980; 2: 97-101.

33. Takeda K, Nakata T, Takesako T, Itoh H, Hirata M, Kawasaki, S, Hayashi J, Oguro M, Sasaki S, Nakagawa M. Sympathetic inhibition and attenuation of spontaneous hypertension by PVN lesions in rats. Brain Res 1991; 543: 296-300.

34. Takenaka K, Sasaki S, Uchida A, Fujita H, Nakamura K, Ichida T, Itoh H, Nakata T, Takeda K, Nakagawa M. GABAB-ergic stimulation in hypothalamic pressor area induces larger sympathetic and cardiovascular depression in spontaneously hypertensive rats. Am J Hypertens 1996; 9: 964-972.

35. Park JB, Jo JY, Zheng H, Patel KP, Stern JE. Regulation of tonic GABA inhibitory function, presympathetic neuronal activity and sympathetic outflow from the paraventricular nucleus by astroglial GABA transporters. J Physiol 2009; 587: 4645-4660.

36. Johannessen CU. Mechanisms of action of valproate: a commentatory. Neurochem Int 2000; 37: 103-110.

37. Löscher W. Basic pharmacology of valproate: a review after 35 years of clinical use for the treatment of epilepsy. CNS Drugs 2002; 16: 669-694.

38. Owens MJ, Nemeroff CB. Pharmacology of valproate. Psychopharmacol Bull 2003; 37: 17-24.

39. Perucca E. Pharmacological and therapeutic properties of valproate: a summary after 35 years of clinical experience. CNS Drugs 2002; 16: 695-714.

40. Rosenberg G. The mechanisms of action of valproate in neuropsychiatric disorders: can we see the forest for the trees? Cell Mol Life Sci 2007; 64: 2090-2103.

41. Terbach N, Williams RSB. Structure–function studies for the panacea, valproic acid. Biochem Soc Trans 2009; 37: 1126-1132.

42. Cunningham MO, Woodhall GL, Jones RSG. Valproate modifies spontaneous excitation and inhibition at cortical synapses in vitro. Neuropharmacology 2003; 45: 907-917.

43. Palmer JE, Chronicle EP, Rolan P, Mulleners WM. Cortical hyperexcitability is cortical under-inhibition: evidence from a novel functional test of migraine patients. Cephalalgia 2000; 20: 525-532.

44. Kee HJ, Sohn IS, Nam KI, Park JE, Qian YR, Yin Z, Ahn Y, Jeong MH, Bang YJ, Kim N et al. Inhibition of histone deacetylation blocks cardiac hypertrophy induced by angiotensin II infusion and aortic banding. Circulation 2006; 113: 51-59.

45. Kang SH, Seok YM, Song MJ, Lee HA, Kurz T, Kim I. Histone deacetylase inhibition attenuates cardiac hypertrophy and fibrosis through acetylation of mineralocorticoid receptor in spontaneously hypertensive rats. Mol Pharmacol 2015; 87: 782-791.